

Oxidative Cleavage of β -O-4 Bonds in Lignin Model Compounds with a Single-atom Co Catalyst

Received 00th January 20xx,
Accepted 00th January 20xx

Sijie Liu,^{a,b} Lichen Bai,^c Antoine P. van Muyden,^a Zhangjun Huang,^a Xinjiang Cui,^a Zhaofu Fei,^a Xuehui Li,^{*b} Xile Hu^{*c} and Paul J. Dyson^{*a}

DOI: 10.1039/x0xx00000x

www.rsc.org/

Single-atom catalysts are emerging as the primary catalysts for many reactions due to their 100% utilization of active metal centers leading to high catalytic efficiencies. Herein, we report the use of a single-atom Co catalyst for the oxidative cleavage of the β -O-4 bonds of lignin model compounds at a low oxygen pressure. Under the optimized reaction conditions conversion of 2-(2-methoxyphenoxy)-1-phenylethanol up to 95 % with high selectivities were achieved with a variety of substrates investigated. The reusability of the Co catalyst with the high catalytic efficiency indicate its potential application in the oxidative cleavage of C-O bonds.

Introduction

As the second largest component in lignocellulose, lignin is an attractive renewable source of aromatic building blocks for the chemical and associated industries.¹⁻³ A number of approaches including hydrogenolysis,^{4,5} fast pyrolysis,⁶ hydrolysis,^{5,7-8} and enzymolysis⁹ have been used to obtain aromatic products from lignin. Oxidative pathways are also appealing because they provide access to different products such as dicarboxylic acids and quinines,¹⁰ which represent key chemical building blocks.¹⁰ In oxidative reactions, the commonly used oxidants are chlorine,¹¹ hydrogen peroxide,¹² ozone¹³ and oxygen.^{14,15} Among these oxidants, oxygen is considered to be the most sustainable since only water is generated as a by-product.¹⁰

Cleavage of β -O-4 type bonds in discrete molecular compounds is frequently studied as the first step in the development of new catalysts for the valorization of lignin. Because it is the most abundant linkage and has a lower bond dissociation energy than the C-C (β -5 and β - β) linkages present in lignin (Fig. 1),^{14, 16-17} or as a direct route in the downstream processing/upgrading of β -O-4 linked dimeric compounds generated from lignin.^{1,10} Indeed, many papers describe the catalytic cleavage of the β -O-4 linkage in lignin model compounds/lignin-derived dimers.^{1,4} For example, the catalytic transformation of 2-phenoxy-1-phenylethanol to phenol,

acetophenone and methyl benzoate was successfully achieved using Pd/CeO₂ as the catalyst in the presence of O₂ in MeOH.¹⁸ Recently, a two-step process has been developed for selective oxidation of β -O-4 lignin model compounds based on VOSO₄ and copper catalysts using O₂.¹⁹ Ionic liquids also promote the aerobic oxidation of phenoxyacetophenone,²⁰ according to the report 2-phenoxyacetophenone is converted to phenol and benzoic acid in 1-octyl-3-methylimidazolium acetate under a mild condition (110°C, 1.5 MPa O₂).²⁰ Despite these impressive achievements towards the catalytic oxidation of β -O-4 bonds, highly efficient catalysts based on earth abundant metals that employ sustainable oxidants could be advantageous.

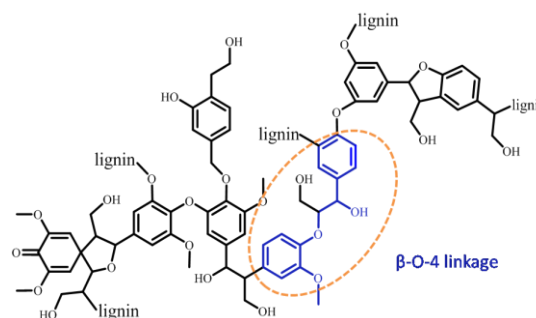


Figure 1 Representative structure of a lignin fragment with β -O-4 linkage.

A class of catalysts that are currently attracting considerable attention are single-atom catalysts (SACs) which combine the single-site nature of homogeneous catalysis with the robustness of a heterogeneous catalyst support.²¹⁻²⁴ In general, SACs comprise mono-dispersed metal atoms stabilized by a specific support, such as defect-rich metal oxides and heteroatom-doped carbon-based materials.²¹ These catalysts are attractive because they exhibit close to 100% atomic efficiency and possess well-defined active sites, which potentially leads to high selectivities and facilitates mechanistic understanding.^{21,22} In addition, SACs are comparatively

^a Institute of Chemical Sciences and Engineering (ISIC), École Polytechnique Fédérale de Lausanne (EPFL), 1015 Lausanne, Switzerland. E-mail: paul.dyson@epfl.ch, Tel: +41 (0)21 693 98 54

^b School of Chemistry and Chemical Engineering, State Key Laboratory of Pulp and Paper Engineering, South China University of Technology, Guangzhou, Guangdong, 510640, China.

^c Laboratory of Inorganic Synthesis and Catalysis, Institute of Chemical Sciences and Engineering, Ecole Polytechnique Fédérale de Lausanne (EPFL), EPFL-ISIC-LSCI, Lausanne, CH 1015 Switzerland.

Electronic Supplementary Information (ESI) available: [ICP data, XRD and TEM of other catalysts, control experiments, figures of effect on reaction time, characterization of recycled catalyst and the NMR of the synthesized lignin model compounds]. See DOI: 10.1039/x0xx00000x

inexpensive and practical since the metal loading is much lower than that used in immobilized nanoparticle catalysts and bulk materials.²²

Despite the rapid development of SACs, to the best of our knowledge, their use in the oxidative cleavage of C-O bonds has not been reported. Herein, we describe the application of a single atom Co catalyst (Co-N-C) in the catalytic (oxidative) cleavage of β -O-4 bonds with the expectation that the Co-N-C catalyst might show similar activity to noble metal (Pt, Pd) SACs,²⁵⁻²⁷ but at a lower cost. In addition, the Co-N-C might be more stable than other non-noble metal SACs (Ni, Cu),²⁸⁻²⁹ and hence any associated toxicity with Co should be minimal. Compared to the other homogeneous and the traditional heterogeneous catalysts, the Co-N-C catalyst displayed superior activity and stability in the oxidative cleavage of model compounds containing β -O-4 bonds.

Results and discussion

Catalyst characterization

The Co-N-C catalyst was prepared by the pyrolysis of $\text{Mg}(\text{OH})_2$ and the $\text{Co}(\text{phen})_2(\text{OAc})_2$ (phen=1,10-phenanthroline) complex according to a literature procedure (see Experimental for full details) which, according to the TEM bright field and dark field images (Fig. 2a and b), has a porous graphic carbon structure absent of any nanoparticles. EDX mapping was recorded in HAADF-STEM mode corresponding to the dark field image (Fig. 2b), which showed that the material mainly consists of homogeneously dispersed C, N, O and Co (Fig. 2c) atoms. Spherical aberration corrected HAADF-STEM (Fig. 2d) was used to observe the atomic resolution imaging of Co atoms (although very small clusters cannot be ruled out). The single Co atoms can be distinguished as well-dispersed bright dots in the HAADF-STEM image (Fig. 2d, in the red cycle), indicative of single-atoms. Co loadings of 3.1 to 3.4wt% was obtained by ICP-AES (Table S1), which is in accordance with previous studies.^{25, 30}

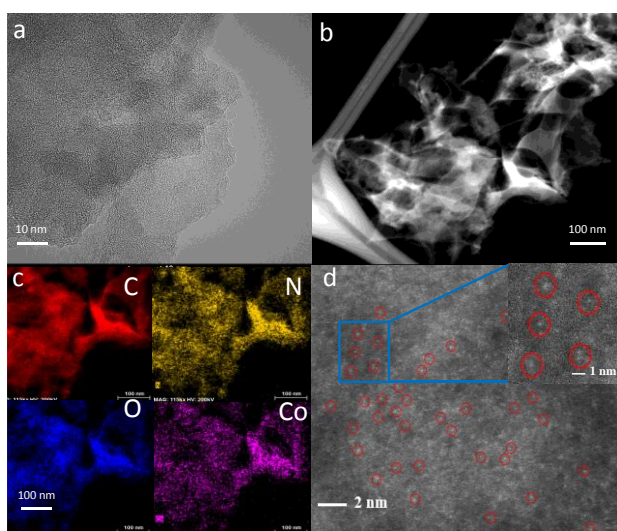


Figure 2 Representative bright filed (a) and dark filed (b) TEM image, EDX mapping images (c) and atomic resolution HAADF-STEM image (d) of the Co-N-C catalyst.

XRD analysis of the Co-N-C catalyst confirms that crystalline MgO and Co nanoparticles are not present as the material gives rise to only broad peaks ($2\theta=28^\circ$) corresponding to amorphous carbon (Fig. 3a). To gain further information on the composition and oxidative state of the catalyst, XPS was performed and confirms the presence of C, N, O and Co in the Co-N-C catalyst (Fig. 3b). The C 1s spectrum shown in Fig. 3c, can be deconvoluted into three peaks and were assigned to the C in C=C double bonds (284.3 eV), C in C=N double bonds (286.2 eV) and C in carboxylic groups (290.3 eV).³¹⁻³² The N 1s spectrum was deconvoluted into three peaks, which were assigned to pyridinic (398.4 eV), graphitic (401.2 eV) and N-oxide (402.8 eV) structures (Fig. 3d).^{25,26} The O 1s spectrum indicates that the presence of O in the catalyst mainly involves C-O single bonds, with a broad peak in 531.2 eV (Fig. 3e). There are also C=O bonds in the catalyst, which has a broad peak in 533.2eV (Fig. 3e). The Co 2p XPS is composed of two main peaks, i.e. Co 2p_{3/2} and Co 2p_{1/2} at 780.7 and 796.3 eV, respectively (Fig. 3f). Combined with two satellite peaks at 785.1 and 801.3 eV (Fig. 3f, blue line), these features imply that the Co is in the 2+ oxidation state.³³

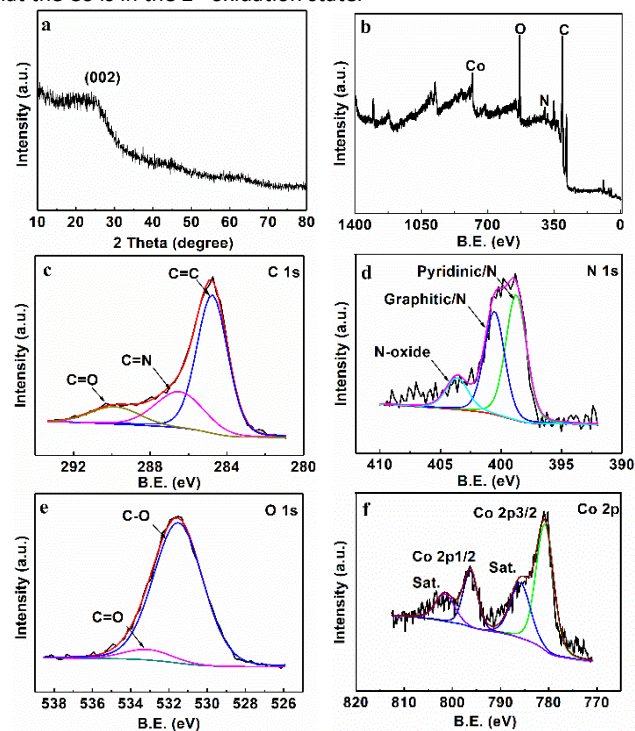


Figure 3 XRD pattern (a) and XPS survey spectrum (b) of the Co-N-C catalyst, and the detailed spectrum for C 1s (c), N 1s (d), O 1s (e) and Co 2p (f).

The SEM image of the Co-N-C catalyst (Fig. S1) reveals that the material is highly porous, possibly as a consequence of etching with nitric acid, with a specific surface area of $322 \text{ m}^2\text{g}^{-1}$ determined by Brunauer-Emmett-Teller (BET) analysis. Although several classes of SACs have been reported, the BET analysis of these materials has not been routinely studied. From the available reports in which the porosity of the SACs was analysed, values range from 220 to $680 \text{ m}^2\text{g}^{-1}$.^{1, 25,26}

Oxidative cleavage of lignin model compound

The oxidative cleavage of 2-(2-methoxyphenoxy)-1-phenylethanol (MPP-ol) in the presence of the Co-N-C catalyst under air was optimized as the reaction can afford guaiacol (G) and/or benzoic acid

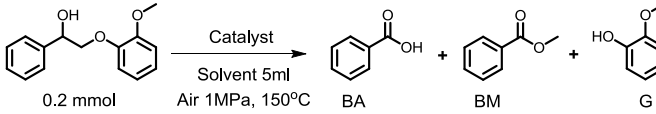
(BA) and also methyl benzoate (BM) when the reaction is conducted in different solvents. MeOH, MeCN and H₂O are widely used as solvents with oxone or O₂ as oxidant in oxidative cleavage of lignin model compounds.^{18-19, 34} In this work, those three solvents were investigated as well using air oxygen as oxidant. Firstly, no reaction was observed in the absence of catalyst in MeOH (Table 1, entry 1). The influence of the solvent was initially investigated in the presence of the Co-N-C catalyst (Table 1, entries 2-7) and MeOH was found to give the highest conversion of MPP-ol of 78% under the reaction conditions (Table 1, entry 2), with G, BM and BA obtained in 45, 30 and 37%, respectively. Low conversions were observed in water and hexane (Table 1, entries 6-7), which is probably due to the low solubility of the substrate in these solvents³⁵. The relatively higher conversion in MeOH than in other solvents indicates that MeOH can react with the generated BA to afford BM and promote the equilibrium to the desired products. To confirm this hypothesis, the corresponding control experiments from BA to BM in MeOH and acetonitrile were carried out in the presence/absence of the catalyst. (Table S2). It was found that BA can be converted to BM in MeOH at high temperatures (150°C) with a moderate conversion of BA (32%) in the absence of catalyst (Table S2, entry 1). Interestingly, the addition of the Co-N-C catalyst improves the conversion only slightly (Table S2, entry 2). However, when MeOH was replaced by CH₃CN, the formation of BM is not observed and only trace quantities of benzamide are detected (by GC-FID). (Table S2, entries 3-4). Thus, the MeOH is both the solvent and a reagent in the reaction.

Single-atom catalysts based on other non-noble metals including Mn, Ni and Cu were also prepared (see Figs. S2-S5 for characterization) and evaluated in the reaction. However, these catalysts are less efficient for the oxidative cleavage of MPP-ol than the Co-N-C catalyst (Table 1, entries 8-10). **The lower activity is probably due to their poorer ability to bind and activate oxygen at a low O₂ pressures (see Scheme 1 for a tentative mechanism).** Control experiments were also performed using homogeneous catalysts, i.e. Co(OAc)₂·4H₂O and Co(OAc)₂·4H₂O with 1,10-phenanthroline, both of which result in lower conversions than the Co-N-C catalyst under the same conditions (Table 1, entries 11-12). For comparison with the Co-N-C, other commonly used oxidative heterogeneous catalysts were also investigated. Co nanoparticles (Co NPs) were synthesized from pure Co-containing metal-organic frameworks according to the reported method³¹ and exhibited a worse activity and selectivity than the Co-N-C catalyst (Table 1, entry 13 vs entry 2). Note that Co nanoparticle impurities in the catalyst also weaken the activity of Co-N-C catalyst (Fig. S6, Table S3, entry 1). Metal oxide catalysts such as Co₃O₄, CuO and CeO₂, which are usually used as catalysts in oxidation of lignin model compounds¹⁰, were also investigated as catalysts for oxidative cleavage of MPP-ol using the same catalytic conditions (Table 1, entries 14-16). Among those three catalysts, Co₃O₄ shows the best activity which attains 59% conversion of MPP-ol, but still less than Co-N-C (Table 1, entry 14 vs entry 2). CuO has the worst activity in this system, which attains only 39% conversion after 4h. Therefore, Co-N-C was selected to the optimized catalyst for this reaction with MeOH as the solvent.

NaOH was added to improve the reaction as it induces the esterification process and improves the cleavage of the β-O-4 bond.^{36,37} In the presence of NaOH (0.2 mmol) the conversion increases from 78 to 95%, and the yield of **G and BM increases to 59**

and 83%, respectively (Table 1, entries 2 and 17) under the same condition. Note that a conversion of 63% is obtained in the presence of NaOH in the absence of the Co-N-C catalyst (Table 1, entry 18). The positive influence of NaOH was confirmed in the control experiment involving the conversion BA to BM (Table S2, entries 5, 6), which is significantly improved in the presence of the base. A conversion of 37% using Co-N-C without NaOH (Table S2, entry 2), and a conversion of 46% using NaOH without Co-N-C (Table S2, entry 5) is boosted to 78% in the presence of both the catalyst and base (Table S2, entry 6). **The effect of solid bases (MgO and CaO)³⁸ was also investigated using MeOH as solvent and the results are given in Table S3 (entries 2 and 3). The conversion of MPP-ol was 81 and 84%, respectively, compared with that using NaOH (95%) under otherwise the same conditions (Table 1, entry 17). The lower activity of the solid bases is probably due to less intimate interactions with the substrates.**

Table 1 Optimization of the reaction conditions. ^a



Entry	Catalyst	Solvent	Conv. (%)	Yield (%) ^b		
				G	BM	BA
1	/	MeOH	2	n.d.	n.d.	n.d.
2	Co-N-C	MeOH	78	45	30	37
3	Co-N-C	MeCN	65	37	n.d.	n.d.
4	Co-N-C	DMF	59	25	n.d.	n.d.
5	Co-N-C	DMSO	36	12	n.d.	n.d.
6	Co-N-C	Hexane	42	24	n.d.	20
7	Co-N-C	H ₂ O	39	22	n.d.	13
8	Mn-N-C	MeOH	48	16	13	10
9	Ni-N-C	MeOH	31	11	8	9
10	Cu-N-C	MeOH	48	17	11	14
11 ^c	Co(OAc) ₂	MeOH	31	11	12	16
12 ^d	Co(OAc) ₂ /L	MeOH	67	30	24	35
13 ^e	Co NPs	MeOH	63	18	25	14
14 ^e	Co ₃ O ₄	MeOH	59	20	21	11
15 ^e	CuO	MeOH	39	14	10	6
16 ^e	CeO ₂	MeOH	48	19	13	7
17 ^f	Co-N-C	MeOH	95	59	83	9
18 ^f	/	MeOH	63	38	47	9

L = 1,10-phenanthroline, n.d. = not detected.

^a Reaction conditions: catalyst (20 mg), substrate (48 mg, 0.2 mmol), solvent (5 ml), air (1 MPa), 150°C, 4 h. ^b Yields were determined by GC-FID.

^c Co(OAc)₂·4H₂O (12 mg). ^d Co(OAc)₂·4H₂O (12 mg), 1,10-phenanthroline (12 mg). ^e Catalyst (20 mg). ^f NaOH (0.2 mmol).

Influence of the reaction temperature and time

In the absence of NaOH, cleavage of β-O-4 bond in MPP-ol is highly temperature-dependent (Fig. 4a, black line). As the temperature is raised from 110°C to 120°C, the conversion sharply increases from 48 to 69%, with the conversion increasing only slightly (to 78%) as the temperature is raised from 120 to 150°C (Fig. 4a, black line). Above 150°C the conversion decreases, presumably due to the condensation of phenolic oligomers.³⁹ In contrast, the Co-N-C catalyst is less sensitive to temperature in the presence of NaOH (Fig.

4a, red line), with a conversion of 88% observed at 110°C, which increases to the maximum value of 95% at 150°C.

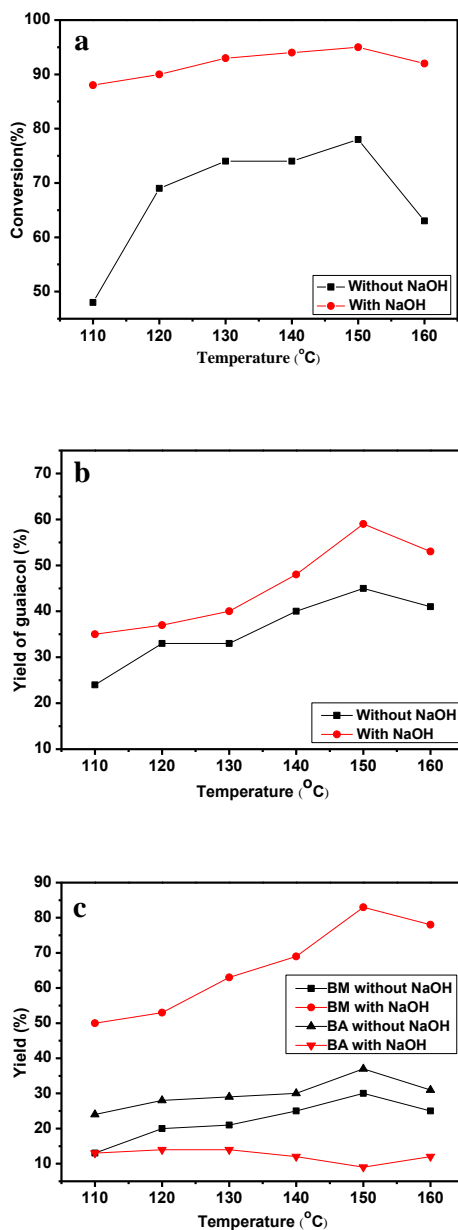


Figure 4 Effect of temperature on (a) 2-(2-methoxyphenoxy)-1-phenylethanone (MPP-ol) conversion, (b) guaicol (G) yield, (c) methyl benzoate (BM) yield and benzoic acid (BA) yield. Reaction conditions: Co-N-C (20 mg), MPP-ol (0.2 mmol), MeOH (5 ml), air (1 MPa), 4 h.

The yield of G gradually increases with temperature irrespective of the NaOH additive (Fig. 4b). Control experiments employing G as the substance demonstrate that G is stable under the reaction conditions (Table S3, entries 4 and 5). G is formed through the cleavage of the C-O bond in β -O-4 model compound (Scheme 1), and higher temperatures favor cleavage of this C-O bond. In the absence of NaOH, the yield of BM and BA increases slightly as the temperature is increased (Fig. 4c, black line), indicating that elevated temperatures promote the cleavage of β -O-4 bond as well as esterification of the BA with MeOH. In the presence of NaOH,

however, the yield of BM increases considerably at the expense of BA, due to the promotion of the esterification under basic conditions.

The conversion of MPP-ol was studied as a function of time with NaOH accelerating the reaction (Fig. S7a), as the base facilitates the fast oxidation of MPP-ol to 2-(2-methoxyphenoxy)-1-phenylethanone (MPP-one).⁴⁰ The maximum yield of the three products is observed after 4 h, with 59, 83 and 9% of G, BM and BA obtained, respectively. The yield of BM in basic conditions reaches stabilization within less than 1 h, further implying fast esterification promoted by NaOH (Fig. S7b, c).

Table S4 lists other catalytic systems employed for the oxidation of MPP-ol reported in recent years. Compared to these catalysts, our system shows several prominent advantages, such as higher activity than a Pd/CeO₂ catalyst¹⁸ at a lower temperature (150°C compared to 185°C) and shorter reaction time (4 vs. 24 h). Homogenous catalysts based on ruthenium and rhenium^{34,41} exhibit similar activity to the Co-N-C catalyst, but are considerably more expensive, as are the ionic liquid-based systems employed in this reaction.^{20,34}

Catalytic oxidation of other lignin model compounds

The oxidative cleavage of other compounds was evaluated under optimized reaction conditions (Table 2). In general, the Co-N-C catalyst exhibits good activity and yield for compounds containing β -O-4 bonds with C $_{\alpha}$ -OH or β -O-4 ketone units (Table 2, entries 1-3), with conversions typically exceeding 80% (Table 2, entries 1-3). The higher conversion obtained for 2-(2-methoxyphenoxy)-1-phenylethanone (MPP-one) compared to MPP-ol indicates that the MPP-ol is initially oxidized into MPP-one (see below, Scheme 1). However, with substrates that do not contain these units in the C $_{\alpha}$ position, conversions are considerably lower, i.e. typically < 20% (Table 2, entry 4), as the β -O-4 alcohol is initially oxidized to β -O-4 ketone which then facilitates the cleavage of C-O bond.¹⁹ Moreover, the Co-N-C catalyst does not efficiently cleave 4-O-5 (Table 2, entry 5) and α -O-4 bonds (Table 2, entries 6, 7). It is known that β -O-4 dimeric model compounds with more functional group and polymeric substrates are structurally more close to true nature-lignin. However, cleavage of the C-O bonds in these model compounds usually requires more harsh conditions such as use of oxygen (O₂)⁴² or hydrogen peroxide (H₂O₂).⁴³⁻⁴⁴ Two more complicated dimeric model compounds 1-(3,4-dimethoxyphenyl)-2-(2-methoxyphenoxy)-propane-1,2-diol (DMPD) and guaicylgly-cerol-guaicyl ether (GGE) were also studied (Table S5). For the DMPD substrate, conversion cannot be detected at 150°C using air as oxidant under otherwise same conditions used for MPP-ol (Table S5, entry 1 vs Table 1, entry 17). By increasing the temperature, low conversion can be observed (Table S5, entries 2-3). Similar phenomena were observed when GGE substrate was used (Table S5, entries 4-6). Only at high temperature (200°C) and by applying pure oxygen, the conversion can be increased significantly for DMPD and GGE to 65% and 48%, respectively (Table 2, entries 8-9). It is obvious that the use of high pressure oxygen is crucial. But even at this harsher condition, the conversion of the dimers DMPD and GGE are lower than that of the MPP-ol. The reduced efficiency for DMPD and GGE is probably due to the stronger steric hindrance in those two compounds, which usually hinder the β -O-4 cleavage in lignin.⁴⁵

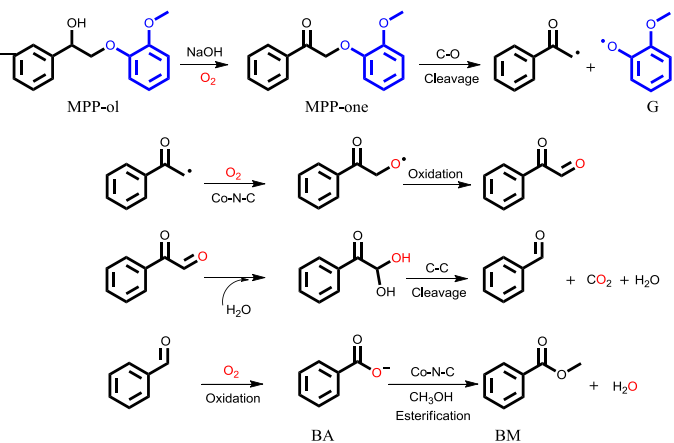
Table 2 Evaluation of the substrate scope of the Co-N-C catalyst.^a

Entry	Substrate	Conv. (%)	Products (% yield) ^b	
1		99		
2		93		
3		82		
4		12		
5		15		/
6		13		
7		14	/	
8 ^c		65		
9 ^c		48		

^a Reaction conditions: Co-N-C (20 mg), NaOH (0.2 mmol), substrate (0.2 mmol), MeOH (5 ml), air (1 MPa), 150°C, 4 h. ^b Yields were obtained by GC-FID. ^c Co-N-C (20 mg), NaOH (0.2 mmol), substrate (0.2 mmol), MeOH (5 ml), O₂ (1 MPa), 200°C, 10h, and the conversion was determined by HPLC.

Proposed mechanism

Based on the experimental data and previous reports^{36, 46-48}, a possible reaction pathway is proposed for the oxidative cleavage of MPP-ol by the Co-N-C catalyst (Scheme 1). In the first step, the MPP-ol is oxidized to MPP-one in the presence of O₂ and NaOH. Then, C-O bond cleavage takes place to generate G and a radical intermediate. In the presence of the Co-N-C catalyst, the radical intermediate can react further with oxygen to form phenylglyoxal.⁴⁶⁻⁴⁷ The C-C bond in phenylglyoxal can then be cleaved to form BA,¹⁸ which subsequently reacts with methanol to generate BM. To support this proposed mechanism, an additional control experiment was conducted with phenylglyoxal, which is converted exclusively to BM (Table S3, entry 6).



Scheme 1 Proposed reaction pathway of MPP-ol.

Recycling experiments

Recycling of the Co-N-C catalyst was studied under the optimized reaction conditions (Fig. 5), demonstrating that it can be repeatedly used with only a slight decrease in activity (the conversion decreases from 95 to 92% over first four cycles and then to 82% over a further four cycles). Moreover, the yield of each product remains largely constant during the first four cycles. TEM images of the catalyst after eight cycles are essentially the same as the pristine Co-N-C catalyst (Fig. S8). However, the XPS surface content of the recycled Co-N-C catalyst reveals that some cobalt has leached from the surface (Table S6), although the oxidation states appear to be unchanged (Fig. S9). Besides that, the catalyst was washed by the MeOH (5×5 mL) after each run, thus the mechanical loss during the separation also resulted in the deactivation of the catalyst.

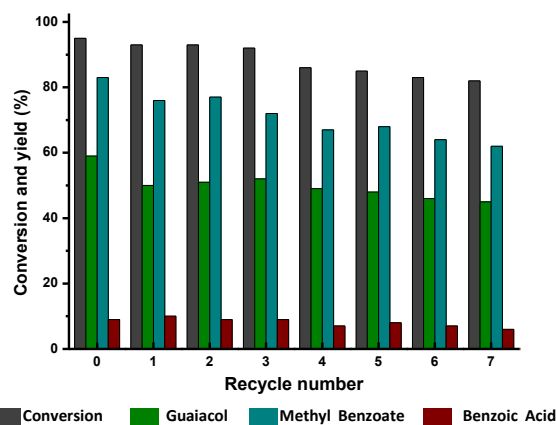


Figure 5 The recyclability Co-N-C catalyst. Reaction conditions: Co-N-C (20 mg), NaOH (0.2 mmol), 2-(2-methoxyphenoxy)-1-phenylethanol (MPP-ol) (0.2 mmol), MeOH (5 ml), air (1 MPa), 150°C, 4 h.

Conclusions

A single-atom Co-N-C catalyst was successfully applied in oxidative cleavage of β-O-4 bond in MPP-ol and other substrates. Under the optimize conditions (150°C, 4 h), 95% conversion of MPP-ol can be attained and the yield of G and BM are 59 and 83%, respectively. By

oxidation of the hydroxyl group in C_{α} , the β -O-4 bond becomes easier to cleave and the combination of the Co-N-C catalyst with NaOH also accelerates the esterification of the in-situ generated BA with MeOH. Furthermore, the Co-N-C catalyst shows good reusability and can be recovered readily using centrifugation and is superior to other catalyst reported for this reaction.

Experimental

Materials and methods

2-(2-methoxyphenoxy)-1-phenylethanol (MPP-ol), 2-(2-methoxyphenoxy)-1-phenylethanone (MPP-one), 2-phenoxy-1-phenylethanol (PP-ol), 2-(2,6-dimethoxyphenoxy)-1-phenylethanol (DMP-ol) and 1-(benzyloxy)-2-methoxybenzene (BMB) were synthesized according to literature methods¹⁹ and the details can be found in SI. All of those synthesized materials were characterized by NMR spectroscopy on a Bruker 400 MHz instrument (Figs. S10-S14). 1-(3,4-dimethoxyphenyl)-2-(2-methoxyphenoxy)-propane-1,2-diol (DMPD), and guaiacylglycerol-guaiacyl ether (GGE), diphenyl ether and 1-phenoxy-2-phenylethane were obtained from commercial sources and used without further purification. **The ¹H NMR spectra of DMPD and GGE are shown in Figs. S15 and S16.**

Preparation of the Co-N-C catalyst

The catalyst was prepared using a modified literature method.^{25,26} $\text{Co}(\text{OAc})_2 \cdot 4\text{H}_2\text{O}$ (125 mg, 0.5 mmol) and 1,10-phenanthroline (270 mg, 1.5 mmol) were dissolved in ethanol (120 mL) and sonicated for 30 minutes. A homogenous solution containing the $\text{Co}(\text{phen})_2(\text{OAc})_2$ complex precursor²⁵ was formed, $\text{Mg}(\text{OH})_2$ (4 g, 69 mmol) was added, and the resulting reaction mixture was sonicated for another 30 min. The resulting suspension was heated at 60°C for 4 h and then the ethanol was removed under vacuum. The solid material was ground into a powder using a ceramic mortar and then pyrolysed at 700°C under N_2 atmosphere for 2 h. The resulting material was stirred in nitric acid (120 mL, 1M) for 2 h to remove the MgO support and any other unsupported metal particles. Further washing with deionized water (3×100 mL) was applied to remove the acid. Other non-noble metal catalysts were synthesized using the same method employing $\text{Mn}(\text{OAc})_2$, $\text{Cu}(\text{OAc})_2 \cdot \text{H}_2\text{O}$ or $\text{Ni}(\text{OAc})_2 \cdot 4\text{H}_2\text{O}$ instead of $\text{Co}(\text{OAc})_2 \cdot 4\text{H}_2\text{O}$.

Catalyst characterization

The morphology of the catalyst was determined on a JEOS JSM 6700F field-emission scanning electron microscope (SEM). Transmission electron microscopy (TEM) was performed on an FEI Talos instrument operated at 200 kV high tension. Energy-dispersive X-ray spectroscopy (EDX) mapping was used for elemental characterization. For atomic resolution spherical aberration corrected imaging, measurements were performed on an FEI Titan Themis 60-300 operated at 200 kV with an aberration-corrected electron probe in high angle annular dark field scanning transmission electron microscopy (HAADF-STEM) mode. The surface area was analysed by N_2 physisorption at 77 K with a Micromeritics ASAP 2000M apparatus. X-ray diffraction (XRD) patterns were recorded on a Bruker Nonius Apex II Advance X-ray diffractometer equipped with a Mo-K α radiation. X-ray photoelectron spectroscopy (XPS) was

recorded on a PHI Versa Probe II scanning X-ray electron spectrometer with Al K α X-ray sourced the curve fitting was performed by the PHI Multipak software. Inductively coupled plasma-atomic emission spectroscopy (ICP-AES) was obtained by a NexIon 350 (Perkin Elmer) instrument. Before dissolving in ultra-pure nitric acid, all the samples were placed in muffle oven to remove the carbon support and ensure all of the metal ions were exposed by heated at 600°C for 6 h in air.

Catalytic reaction

The catalytic reactions are performed according to reference methods.^{18,19} In a typical reaction, the catalyst (20 mg), substrate (0.2 mmol) and MeOH (5 ml) were placed in an autoclave and pressurized to 1 MPa with air. In some reactions, NaOH (0.2 mmol) was added as a co-catalyst before pressurizing with air. The autoclave was heated to the desired temperature for the appropriate time and the contents of the autoclave were stirred. After cooling to room temperature and releasing the pressure, the catalyst was removed by centrifuging (6000 rpm, 10 min.). The reaction products were analysed on an Agilent 7890B gas chromatograph mass spectrometer (GC-MS) equipped with an Agilent 7000C GC-MS triple quad detector and a capillary column (Agilent, 30m×0.25mm×0.25 μm) connected to a flame ionization detector (FID). Dimethyl phthalate was used as the standard. The NaOH co-catalyst was neutralized with aqueous HCl (37wt%) prior to quantification by GC-MS. High performance liquid chromatography (HPLC) were conducted with an Agilent 1200 Series instrument using a reverse-phase Eclipse XDB-C18 column (4.6 × 150 mm, 5 μm , Agilent) and a UV-vis 785A detector set at 260 nm. A mix of water and MeOH (20:80m/m ratio) was used as eluent.

Conflicts of interest

There are no conflicts to declare.

Acknowledgements

We thank the Swiss National Science Foundation (to A.v.M), the European Research Council (no. 681292 to X.L.H), Natural Science Foundation of China (21736003) and the Oversea Study Program of Guangzhou Elite Project for financial support. The Interdisciplinary Center for Electron Microscopy at EPFL for assistance with electron microscopy and XPS, and Dr. Wu Lan, Dr. Florent Héroguel and Prof. Jeremy Luterbacher (EPFL) for help with the N_2 adsorption-desorption measurements.

References

1. J. Zakzeski, P. C. A. Bruijninx, A. L. Jongerius, B. M. Weckhuysen, *Chem. Rev.*, 2010, **110**, 3552-3599.
2. F. G. Calvo-Flores, J. A. Dobado, *ChemSusChem*, 2010, **3**, 1227-1235.
3. Z. Cai, Y. Li, H. He, Q. Zeng, J. Long, L. Wang, X. Li, *Ind. Eng. Chem. Res.*, 2015, **54**, 11501-11510.
4. C. Li, X. Zhao, A. Wang, G. W. Huber, T. Zhang, *Chem. Rev.*, 2015, **115**, 11599-11624.

5. N. Yan, C. Zhao, P. J. Dyson, C. Wang, L. Liu, Y. Kou, *ChemSusChem*, 2008, **1**, 626-629.
6. W. Chen, D. J. McClelland, A. Azarpira, J. Ralph, Z. Luo, G. W. Huber, *Green Chem.*, 2016, **18**, 271-281.
7. H. Ben, W. Mu, Y. Deng, A. J. Ragauskas, *Fuel*, 2013, **103**, 1148-1153.
8. Z. Zhu, M. Sun, C. Su, H. Zhao, X. Ma, Z. Zhu, X. Shi, K. Gu, *Bioresour. Technol.*, 2013, **128**, 229-234.
9. Y. Liu, J. Wang, M. P. Wolcott, *ACS Sustainable Chem. Eng.*, 2016, **4**, 7225-7230.
10. R. Ma, Y. Xu, X. Zhang, *ChemSusChem*, 2015, **8**, 24-51.
11. D. R. Svenson, H. Jameel, H. Chang, J. F. Kadla, *J. Wood Chem. Technol.*, 2006, **26**, 201-213.
12. I. Hasegawa, Y. Inoue, Y. Muranaka, T. Yasukawa, K. Mae, *Energy Fuel*, 2011, **25**, 791-796.
13. A. K. H. Aljibouri, G. Turcotte, J. Wu, C. Cheng, *Energy Sci. Eng.*, 2015, **3**, 541-548.
14. F. S. Chakar, A. Ragauskas, *Ind. Crops Prod.*, 2004, **20**, 131-141.
15. M. V. Galkin, S. Sawadjoon, V. Rohde, M. Dawange, J. S. M. Samec, *ChemCatChem*, 2014, **6**, 179-184.
16. A. Beste, A. C. Buchanan, *J. Org. Chem.*, 2009, **74**, 2837-2841.
17. S. Kim, S. C. Chemly, M. R. Nimlos, Y. J. Bomble, T. D. Foust, R. S. Paton, G. T. Beckham, *J. Phys. Chem. Lett.*, 2011, **2**, 2846-2852.
18. W. Deng, H. Zhang, X. Wu, R. Li, Q. Zhang, Y. Wang, *Green Chem.*, 2015, **17**, 5009-5018.
19. M. Wang, J. Lu, X. Zhang, L. Li, H. Li, N. Luo, F. Wang, *ACS Catal.*, 2016, **6**, 6086-6090.
20. Y. Yang, H. Fan, Q. Meng, Z. Zhang, G. Yang, B. Han, *Chem. Comm.*, 2017, **53**, 8850-8853.
21. X. Yang, A. Wang, B. Qiao, J. Li, J. Liu, T. Zhang, *Acc. Chem. Res.*, 2013, **46**, 1740-1748.
22. S. Liang, C. Hao, Y. Shi, *ChemCatChem*, 2015, **7**, 2559-2567.
23. B. Zhang, H. Asakura, J. Zhang, S. De, N. Yan, *Angew. Chem. Int. Ed.*, 2016, **55**, 8319-8323.
24. Z. Zhang, Y. Zhu, H. Asakura, B. Zhang, J. Zhang, M. Zhou, Y. Han, T. Tanaka, A. Wang, T. Zhang, N. Yan, *Nat. Commun.*, 2017, **8**, 16100.
25. W. Liu, L. Zhang, W. Yan, X. Liu, X. Yang, S. Miao, W. Wang, A. Wang, T. Zhang, *Chem. Sci.*, 2016, **7**, 5758-5764.
26. M. Li, S. Wu, X. Yang, J. Hu, L. Peng, L. Bai, Q. Huo, J. Guan, *Appl. Catal. A*, 2017, **543**, 61-66.
27. F. Pan, H. Zhang, K. Liu, D. Cullen, K. More, M. Wang, Z. Feng, G. Wang, G. Wu, Y. Li, *ACS Catal.*, 2018, **8**, 3116-3122.
28. J. Xie, K. Yin, A. Serov, K. Artyushkova, H. N. Pham, X. Sang, R. R. Unocic, P. Atanassov, A. K. Datye, R. J. Davis, *ChemSusChem*, 2017, **10**, 359-362.
29. X. Li, X. Huang, S. Xi, S. Miao, J. Ding, W. Cai, S. Liu, X. Yang, H. Yang, J. Gao, J. Wang, Y. Huang, B. Liu, *J. Am. Chem. Soc.*, 2018, **140**, 12469-12475.
30. X. Sun, A. I. Olivos-Suarez, D. Osadchii, M. J. V. Romero, F. Kapteijn, J. Gascon, *J. Catal.*, 2018, **357**, 20-28.
31. P. Yin, T. Yao, Y. Wu, L. Zheng, Y. Lin, W. Liu, H. Ju, J. Zhu, X. Hong, Z. Deng, G. Zhou, S. Wei, Y. Li, *Angew. Chem. Int. Ed.*, 2016, **55**, 10800-10805.
32. M. Wang, J. Han, Y. Hu, R. Guo, *RSC Adv.*, 2017, **7**, 15513-15520.
33. D. Singh, I. I. Soykal, J. Tian, D. von Deak, J. King, J. T. Miller, U. S. Ozkan, *J. Catal.*, 2013, **304**, 100-111.
34. B. Zhang, C. Li, T. Dai, G. W. Huber, A. Wang, T. Zhang, *RSC Adv.*, 2015, **5**, 84967-84973.
35. Q. Song, F. Wang, J. Cai, Y. Wang, J. Zhang, W. Yu, J. Xu, *Energy Environ. Sci.*, 2013, **6**, 994-1007.
36. M. Wang, J. Lu, L. Li, H. Li, H. Liu, F. Wang, *J. Catal.*, 2017, **348**, 160-167.
37. V. M. Roberts, V. Stein, T. Reiner, A. Lemonidou, X. Li, J. A. Lercher, *Chem. Eur. J.*, 2011, **17**, 5939-5948.
38. R. Chaudhary, P. L. Dhepe, *Green Chem.*, 2017, **19**, 778-788.
39. J. Long, Y. Xu, T. Wang, Z. Yuan, R. Shu, Q. Zhang, L. Ma, *Appl. Energ.*, 2015, **141**, 70-79.
40. K. Kervinen, H. Korpi, M. Leskela, T. Repo, *J. Mol. Catal. A: Chem.*, 2003, **203**, 9-19.
41. W. Huo, W. Li, M. Zhang, W. Fan, H. Chang, H. Jameel, *Catal. Lett.*, 2014, **144**, 1159-1163.
42. L. Hdidou, K. Khallouk, A. Solhy, B. Manoun, A. Oukarroum, A. Barakat, *Catal. Sci. Technol.*, 2018, **8**, 5445-5453.
43. M. Halma, D. Lachenal, N. Marlin, A. Deronzier, M. C. Brochier, M. Zarubin, *Ind. Crop Prod.*, 2015, **74**, 514-522.
44. H. Lange, S. Decina, C. Crestini, *Eur. Polym. J.*, 2013, **49**, 1151-1173.
45. T. Dizhbite, G. Telysheva, V. Jurkjane, U. Viesturs, *Bioresour. Technol.*, 2004, **95**, 309-317.
46. B. Karimi, S. Abedi, J. H. Clark, V. Budarin, *Angew. Chem. Int. Ed.*, 2006, **45**, 4776-4779.
47. M. Wang, F. Wang, J. Ma, M. Li, Z. Zhang, Y. Wang, X. Zhang, J. Xu, *Chem. Commun.*, 2014, **50**, 292-294.
48. L. Zhang, X. Bi, X. Guan, X. Li, Q. Liu, B. D. Barry, P. Liao, *Angew. Chem. Int. Ed.*, 2013, **52**, 11303-11307.